Progress In Electromagnetics Research C, Vol. 34, 41–52, 2013

A THREE-BAND T-JUNCTION POWER DIVIDER BASED ON ARTIFICIAL TRANSMISSION LINES

G. Monti*, R. de Paolis, and L. Tarricone

Innovation Engineering Department, University of Salento, Via per Monteroni, Lecce 73100, Italy

Abstract—Based on the Composite Right/Left-Handed (CRLH) Transmission Line (TL) approach this paper presents a 3-band T-Junction power divider. The proposed design strategy uses a stub-loaded TL for the right-handed portion of the line; this way, with respect to a conventional CRLH line, one more degree of freedom is available. Experimental and numerical results referring to a prototype using surface-mount capacitors and inductors are reported and discussed. It is demonstrated that the artificial transmission line (ATL) here presented is an optimum candidate for designing high-added value microwave devices. Furthermore based on the use of metal-insulator-metal capacitors and short circuited stubs, a monolithic implementation is also proposed.

1. INTRODUCTION

Composite Right/Left-Handed (CRLH) Artificial Transmission Lines (ATLs) [1–5] are the TL implementation of a Double Negative medium [6–11], usually implemented by loading a conventional TL with a high-pass network.

Due to their unusual dispersion properties, CRLH ATLs have attracted widespread interest in recent years [1–5, 12–19], and several applications, such as dual-band components [2, 14, 15], have already been proposed.

In the present work the use of a Purely Right-Handed (PRH) ATL for the RH portion of the CRLH line is suggested; it is demonstrated that the proposed design approach adds one more degree of freedom that can be exploited to improve the performance of common microwave devices.

Received 17 September 2012, Accepted 19 October 2012, Scheduled 25 October 2012

* Corresponding author: Giuseppina Monti (giuseppina.monti@unisalento.it).

As a proof of concept of the advantages related to the proposed design strategy, a three-band T-Junction power divider (TJ-PWD) is presented. Experimental results referring to a prototype using surface-mount technology for the lumped inductors/capacitors and working at (0.9 GHz, 1.62 GHz, 2.7 GHz) are presented and discussed. Furthermore, a compact and monolithic implementation of the CRLH ATL based on the use of Metal Insulator Metal (MIM) capacitors combined with short-circuited/open-ended stubs is also proposed.

The paper is structured as follows: Section 2 introduces the ATL concept. Later on, Section 3 presents the proposed three-band TJ-PWD. Finally, some conclusions are drawn in Section 4.

2. ARTIFICIAL TRANSMISSION LINE

Artificial Transmission Lines (ATLs) are periodic networks designed by loading a conventional TL with lumped or distributed elements. Providing that the phase shift corresponding to the unit cell satisfies the condition:

$$\phi_{\text{unit\_cell}} \ll 2\pi \tag{1}$$

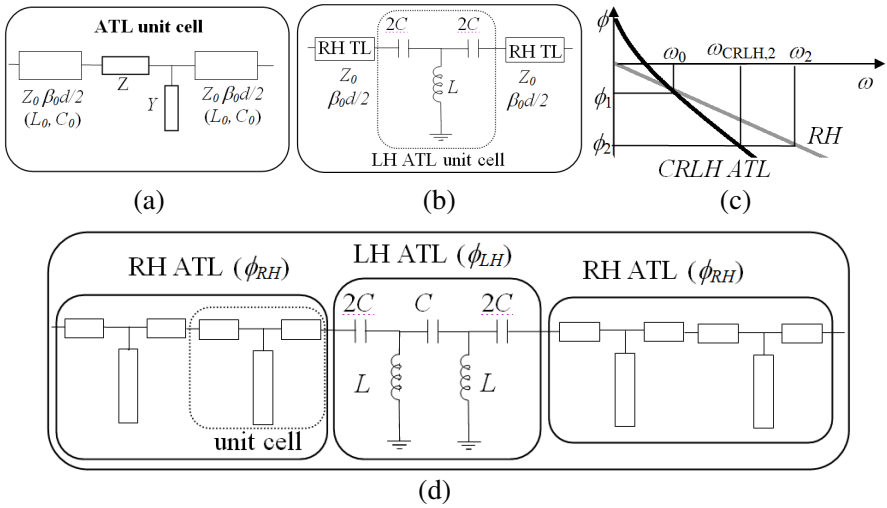

Figure 1. Examples of unit cell that can be used for designing an artificial transmission line: (a) PRH unit cell, (b) CRLH unit cell, (c) phase response of a PRH ATL and a CRLH ATL with the same electrical length at ω_0, (d) proposed CRLH unit cell.

the line exhibits an effectively homogeneous behavior described by the following effective parameters (see Figure 1(a)):

$$\begin{aligned} Z_{\mathrm{ATL}} &= \sqrt{\frac{Z'}{Y'}} = \sqrt{\left(L_0 + \frac{Z}{j\omega d}\right) \Big/ \left(C_0 + \frac{Y}{j\omega d}\right)}, \\ \beta_{\mathrm{ATL}} &= \sqrt{-Z'Y'} = \omega\sqrt{\left(L_0 + \frac{Z}{j\omega d}\right)\left(C_0 + \frac{Y}{j\omega d}\right)}. \end{aligned} \tag{2}$$

From (2) one can derive that Z and Y can be fixed to have a Purely Right (PRH) or a Composite Right/Left-Handed (CRLH) behaviour.

More specifically, loading elements in a low-pass topology correspond to a PRH behaviour, whilst a high-pass topology must be used to achieve a CRLH behaviour.

Figure 1(a) illustrates an example of unit cell that can be used for designing a PRH ATL, it consists of a conventional TL loaded with an open-ended stub. The corresponding effective parameters are given by [15–18]:

$$\begin{aligned} Y = \frac{jtg\,(\theta_s)}{Z_s} \Rightarrow Z_{0\mathrm{ATL}} &= \sqrt{\frac{L_0}{\left(C_0 + \frac{tg(\theta_s)}{\omega d Z_s}\right)}} \approx \sqrt{\frac{L_0}{\left(C_0 + \frac{d_s}{d}C_s\right)}}, \\ \varphi_{\mathrm{ATL}} = Nd\omega_0\sqrt{L_0\left(C_0 + \frac{tg\,(\theta_s)}{\omega d Z_s}\right)} &\approx Nd\omega_0\sqrt{L_0\left(C_0 + \frac{d_s}{d}C_s\right)}. \end{aligned} \tag{3}$$

where Z_s and θ_s are the characteristic impedance and the electrical length of the loading stub. L_0, C_0, and d are the distributed parameters and the physical length of the loaded TL, while L_s, C_s, and d_s are the same quantities referred to the loading stub. The approximately equal sign in (3) refers to the case of a loading stub with a physical length satisfying the condition $d_s \ll \lambda$.

As for a CRLH line, a possible unit cell is illustrated in Figure 1(b); providing that the balanced condition ($Z_{\mathrm{RH}} = Z_0 = Z_{\mathrm{LH}} \Rightarrow \sqrt{L_0 C} = \sqrt{L C_0}$) is satisfied, the following effective parameters can be derived:

$$\begin{aligned} Z_{\mathrm{CRLH}} &= \sqrt{\frac{L_0}{C_0}} = \sqrt{\frac{L}{C}}, \\ \beta_{\mathrm{CRLH}} &= \sqrt{\omega^2 L_0 C_0 - \frac{1}{\omega^2 L' C'}}, \quad \{C' = Cd,\ L' = Ld\} \end{aligned} \tag{4}$$

From (4) it is evident that three degrees of freedom are available, consequently the parameters which appear in (4) can be fixed to achieve a dual-band behaviour [2, 14, 15]. In fact, it is well known

that a conventional TL has only two degrees of freedom: the line characteristic impedance, Z_0, and the line electrical length, βd. As a consequence, by using conventional TLs, if a device is designed to work at f_0 (f_1) the first useful upper band is automatically centred at $3f_0$ (f_2). Conversely, by using CRLH TLs, a dual-band behaviour can be obtained by arbitrarily shifting the second working band to a desired frequency.

The design approach here proposed consists in designing the RH portion of the CRLH line as a PRH-ATL (see Figure 1(d)); this way, a further degree of freedom is available which can be exploited to have a three-band behaviour. Referring to Figure 1(d), this can be achieved by fixing the ATL parameters so to satisfy the following equations:

$$\begin{cases} Z_{\mathrm{LH}} = Z_{0\mathrm{ATL}} = Z_a \Rightarrow \sqrt{\frac{L_0}{\left(C_0 + \frac{tg(\theta_s)}{2\pi f dZ_s}\right)}} \approx \sqrt{\frac{L_0}{\left(C_0 + \frac{d_s}{d}C_s\right)}} = \sqrt{\frac{L}{C}} = Z_a \\ \left\{ \frac{M}{2\pi f_1 \sqrt{LC}} - Nd2\pi f_1 \sqrt{L_0\left(C_0 + \frac{d_s}{d}C_s\right)} \right\} = \phi_{\mathrm{CRLH}}(f_1) \hat{=} \phi_1 \\ \left\{ \frac{M}{2\pi f_2 \sqrt{LC}} - Nd2\pi f_2 \sqrt{L_0\left(C_0 + \frac{d_s}{d}C_s\right)} \right\} = \phi_{\mathrm{CRLH}}(f_2) \hat{=} \phi_2 \\ \left\{ \frac{M}{2\pi f_3 \sqrt{LC}} - Nd2\pi f_3 \sqrt{L_0\left(C_0 + \frac{d_s}{d}C_s\right)} \right\} = \phi_{\mathrm{CRLH}}(f_3) \hat{=} \phi_3 \end{cases}, \quad (5)$$

$$\Rightarrow \begin{cases} L = Z_a^2 C, \quad L_0 = Z_a^2\left(C_0 + \frac{d_s}{d}C_s\right) \\ \left(C_0 + \frac{d_s}{d}C_s\right) = \frac{\phi_1 f_1 - \phi_2 f_2}{2\pi N Z_a d\left(f_2^2 - f_1^2\right)} \\ C = \frac{M\left(f_2^2 - f_1^2\right)}{2\pi Z_a f_1 f_2 (\phi_1 f_2 - \phi_2 f_1)} \\ f_2 f_1(\phi_2 f_1 - \phi_1 f_2) + f_3 f_1(\phi_1 f_3 - \phi_3 f_1) + f_3 f_2(\phi_3 f_2 - \phi_2 f_3) = 0 \end{cases}. \quad (6)$$

where M and N are the number of unit cells of the RH- and the LH-ATL, respectively (referring to Figure 1(d), M is equal to 4 and N is equal to 2). As an example of application of the proposed approach, Equation (6) can be used to add a useful working band between the first and the second band corresponding to a conventional TL. Referring to a device requiring a TL with a phase shift of:

$$(2k+1)|\phi|$$

being k an integer number, by using a conventional TL, the first two useful bands are centered at f_1 and f_2 given by:

f_1: $\phi_{\mathrm{TL},1}(f_1) = -|\phi| \Rightarrow f_2 = 3f_1$ corresponding to $\phi_{\mathrm{TL},2}(f_2) = -3|\phi|$

By using the proposed CRLH-ATL a band can be added between f_1 and f_2 by fixing the line phase shift as follows:

$$\phi_{\mathrm{CRLH},i} = \phi_{\mathrm{CRLH}}\left(f_{\mathrm{CRLH},i}\right) = \left[2\left(2-i\right)+1\right]\left|\phi\right|, \quad i = 1,2,3 \tag{7}$$

In fact, by using (7) in (6) and by fixing $f_{\mathrm{CRLH},1} = f_1$, $f_{\mathrm{CRLH},3} = f_2 = 3f_1$, it can be found that the proposed CRLH line has a further useful band centered at $f_{\mathrm{CRLH},2} \approx 1.67f_1$. Alternatively, a band can be added at $f_{\mathrm{CRLH},2} \approx 1.8f_1$ if the line phase shift is fixed as follows:

$$\phi_{\mathrm{CRLH},i} = \phi_{\mathrm{CRLH}}\left(f_{\mathrm{CRLH},i}\right) = \left[2\left(1-i\right)+1\right]\left|\phi\right|, \quad i = 1,2,3 \tag{8}$$

Based on the proposed CRLH-ATL, in the next section a three-band TJ-PWD is presented.

3. THREE-BAND T-JUNCTION POWER DIVIDER

As a proof of concept of the proposed approach, in this section we present a three-band TJ-PWD. The schematic of a conventional TJ is illustrated in Figure 2. It is a three-port network usually employed to split the power applied at port 1 or to combine that applied at port 2 and 3. The approach here suggested consists in substituting the $(-90°)$-RH line with a CRLH one. A similar solution has been already adopted in [12], where a CRLH designed to have a phase shift of $+90°$ has been used to achieve a size reduction. In this paper, the use of a CRLH-ATL based on the design approach described in the previous section is suggested, thus resulting in a three-band behaviour. More specifically, we replaced the $(-90°)$-RH line of a conventional TJ-PWD with the CRLH-ATL illustrated in Figure 1(d) which consists of 4 RH-ATL unit cells and 2 LH-ATL unit cells. The selected operating frequencies were: 0.9 GHz, 1.62 GHz, 2.7 GHz. According to the desired three-band behavior, the parameters of the line were

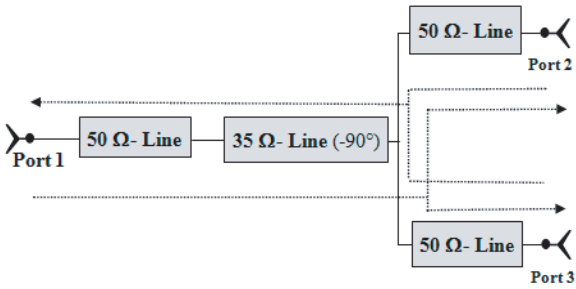

Figure 2. Schematic representation of a conventional T-Junction power divider.

fixed by using Equation (6) so to satisfy the following conditions:

$$\begin{aligned}
&S_{11,35\,\Omega} < -20\,\text{dB}, \quad f \in [800, 3000]\ \text{MHz} \\
&\text{Phase}\,(S_{21}) = [2\,(1-i)+1]\,\frac{\pi}{2}, \\
&@ \\
&(f_{i=1} = 0.9\,\text{GHz},\ f_{i=2} = 1.8 f_1 = 1.62\,\text{GHz},\ f_{i=3} = 3 f_1 = 2.7\,\text{GHz}) \\
\Rightarrow &\left\{\text{Phase}(S_{21})@0.9\,\text{GHz} = \frac{\pi}{2}\right\},\ \left\{\text{Phase}(S_{21})@1.62\,\text{GHz} = -\frac{\pi}{2}\right\}, \\
&\left\{\text{Phase}\,(S_{21})\,@2.7\,\text{GHz} = -3\frac{\pi}{2}\right\}
\end{aligned} \tag{9}$$

where $S_{11,35\,\Omega}$ is the line return loss referred to a 35 Ω-TL. Values calculated this way for the parameters of the CRLH-TL were optimized by means of a microwave circuital simulator resulting in the layout and the values of the lumped elements illustrated in Figure 3; the corresponding $S_{11,35\,\Omega}$ calculated by means of circuital simulations is given in Figure 4. It is evident that, with respect to a 35 Ω impedance, the CRLH ATL of Figure 3 exhibits a good level of matching over the entire frequency range of interest (i.e., [0.9, 2.7] GHz).

As for the scattering parameters of the TJ-PWD, results calculated by means of circuital simulations are summarized in Figure 5; the presence of an additional operating band that falls between the first and the second band corresponding to a conventional TJ-PWD can be noticed.

Furthermore, from comparisons given in Figure 5, it can be noticed that the proposed TJ-PWD exhibits performance similar to the one corresponding to a conventional TJ-PWD (see Figure 2). In fact, in

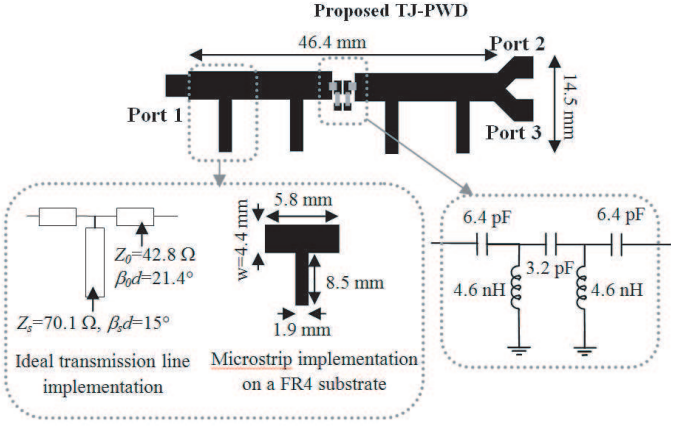

Figure 3. Proposed three-band TJ-PWD.

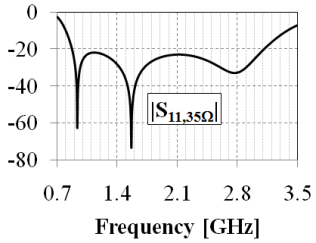

Figure 4. Reflection coefficient of the CRLH ATL illustrated in Figure 3 calculated by using a reference impedance of 35 Ω.

all the three operating bands the reflection coefficient is lower than −20 dB and the transmission coefficient between the two output ports ($|S_{32}|$) is of about −6 dB. As for the occupied area, due to the presence of the loading stubs, it is slightly larger than that occupied by the TJ-PWD of Figure 2, and become approximately the same by bending the stubs.

In order to demonstrate the reliability of these results, a prototype was realized by using surface-mount technology for the LH portion of the ATL (see Figure 6). More specifically, Accu-P 0402 Capacitors and Accu-L 0603 Inductors by AVX Corporation were used. The values given in Figure 3 for the lumped capacitors and inductors were approximated with the ones available in our kit (see Figure 6(a)). As for the RH-ATL unit cell, it was firstly optimized to work with the CRLH line illustrated in Figure 6(a) and then implemented in microstrip technology on a FR4 double-sided copper clad laminate (ε_r = 3.9, $\tan(\delta)$ = 0.019, thickness = 1.6 mm). A photograph of the three-band TJ-PWD prototype is given in Figure 6(b); the corresponding measured scattering parameters and insertion loss are given in Figures 7 and 8, respectively. With respect to simulation results given in Figure 5, a shift of the three operating bands towards higher frequency can be observed. This shift is highlighted in Figures 7(c) and 7(d) where the measured scattering parameters are compared with simulated data; from measurements the three operating bands are centered at: 1.11 GHz, 2.0 GHz, 3.1 GHz. This shift is due to the parasitic effects related to the soldering process of the SMD devices and to the difference between the values of the capacitors calculated by means of circuital simulation and the ones used for the realization. However, from Figures 7–8 an excellent behaviour can be observed in the three operating bands with an insertion loss in the range [0.5, 1.5] dB.

Finally, the TJ-PWD was implemented as a monolithic device by using MIM capacitors and short-circuited stubs for the inductors. The

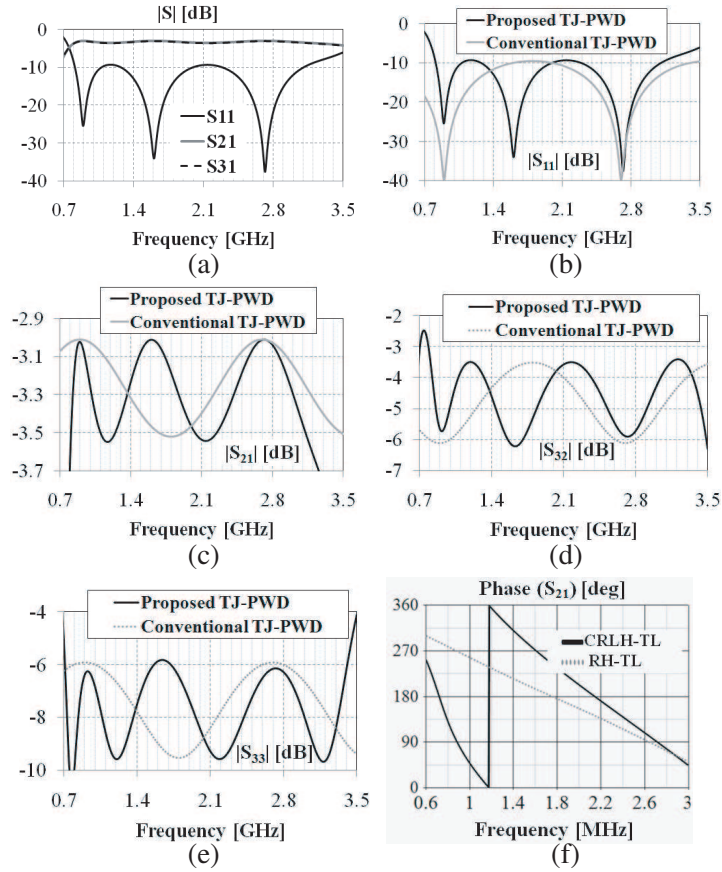

Figure 5. (a) Scattering parameters of the TJ-PWD illustrated in Figure 3. (b)–(e) Comparison between the scattering parameters calculated for a conventional TJ-PWD (see Figure 2) and the ones corresponding to the proposed TJ-PWD: (b) reflection coefficient at the input port (port 1), (c) transmission coefficient between port 1 and 2 ($|S_{21}|$), (d) transmission coefficient between the output ports ($|S_{32}|$), (e) reflection coefficient at the output port 3 ($|S_{33}|$). (f) Comparison between the phase response of a conventional TL with a phase-shift of $-90°$ at 0.9 GHz and the one corresponding to CRLH line illustrated in Figure 3.

design was performed on a silicon substrate ($\varepsilon_r = 11.9$, $h = 525\,\mu$m); the insulator used in designing the MIM capacitors is a 90 nm thick Low Temperature Oxide (LTO) with a relative electric permittivity equal to 4. The layout achieved in this way is illustrated in Figure 9; the occupied area is approximately the same of a conventional TJ-

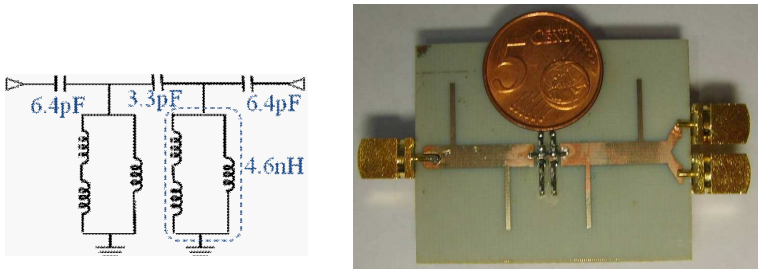

(a) (b)

Figure 6. Realized prototype: (a) values of the SMD devices used for the implementation of the LH portion of the CRLH-ATL, (b) photograph of the fabricated prototype.

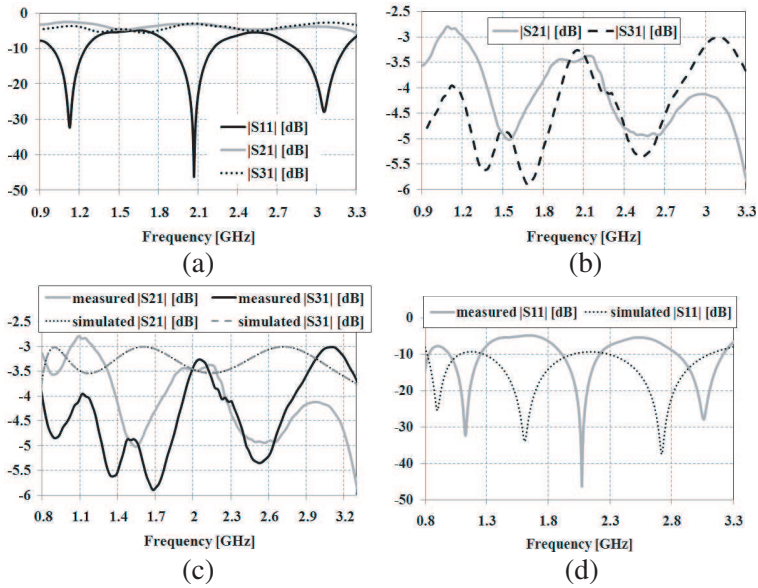

Figure 7. (a), (b) Experimental data obtained for the scattering parameters of the prototype illustrated in Figure 5(b). (c), (d) Comparison between simulated and experimental data.

PWD. More specifically, the area of the proposed device is of about $(3.5 \times 17.2)\,\mathrm{mm}^2$, whereas the one corresponding to a conventional $\lambda/2$ TJ-PWD on the same substrate is of about $(2 \times 30.8)\,\mathrm{mm}^2$.

In order to verify the TJ-PWD behaviour, full-wave simulations were performed with the ADS-Momentum (Agilent) simulator. The corresponding scattering parameters are illustrated in Figure 9: good performance can be observed at the three operating frequencies, thus

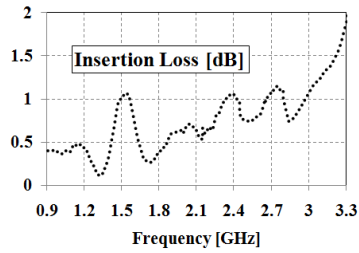

Figure 8. Insertion loss of the proposed TJ-PWD calculated from measurements performed for the prototype illustrated in Figure 6(b).

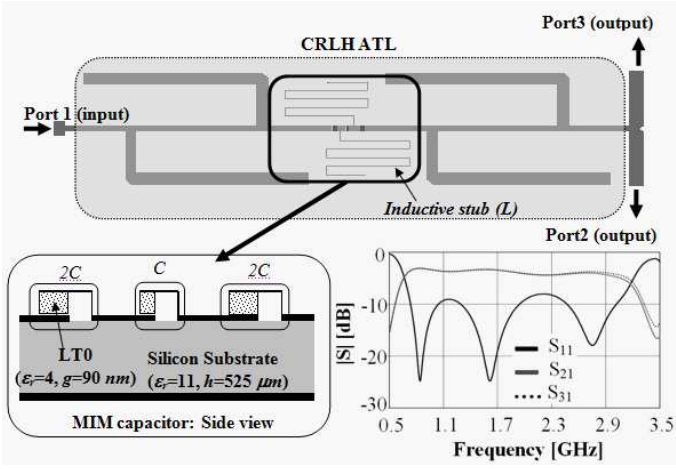

Figure 9. Layout and simulated scattering parameters of the proposed monolithic TJ-PWD (the side view of the MIM capacitors employed in designing the CRLH line is highlighted in the inset).

confirming results obtained with the SMD-based prototype. It is worth underlining that, with respect to the implementation based on SMD devices, the use of MIM capacitors and stubs inductors combines the well-known benefits of the monolithic technology on high resistivity silicon substrate to the advantages of avoiding undesired parasitic effects related to the soldering process and to the approximated values of capacitors and inductors.

4. CONCLUSION

A novel design approach for CRLH transmission lines has been presented. The proposed design strategy uses an artificial transmission line implementation for both the RH and the LH portions of the line. It

has been demonstrated that, with respect to a conventional CRLH line, this strategy adds one more degree of freedom that can be exploited to improve the performance of common microwave devices.

In order to validate the proposed approach, a very compact three-band T-Junction power divider has been presented. Numerical and experimental results, related to a prototype employing surface mounted devices and working at 0.9 GHz, 1.62 GHz, and 2.7 GHz, have been reported and discussed, thus demonstrating the reliability of the proposed approach. Furthermore, based on the use of MIM capacitors and short-circuited/open-ended stubs, a monolithic implementation of the same structure has also been presented. Both implementations of the T-Junction power divider (the monolithic and the one realized using surface-mount technology), are characterized by a very compact size and exhibit a good performance in terms of scattering parameters.

As a result, the advantages highlighted in this paper lead to the conclusion that the proposed artificial transmission line is an optimum candidate for designing high added-value microwave devices.

REFERENCES

1. Caloz, C. and T. Itoh, "Application of the transmission line theory of left-handed (LH) materials to the realization of a microstrip LH line," *IEEE AP-S Symp.*, 412–415, Jun. 2002.
2. Lin, I-H., M. de Vincentis, C. Caloz, and T. Itoh, "Arbitrary dual-band components using composite right/left-handed transmission lines," *IEEE Trans. on Microwave Theory Tech.*, Vol. 52, 1142–1149, 2004.
3. Monti, G., R. de Paolis, and L. Tarricone, "Design of a 3-state reconfigurable CRLH transmission line based on MEMS switches," *Progress In Electromagnetics Research*, Vol. 95, 283–297, 2009.
4. Lai, A., K. M. K. H. Leong, and T. Itoh, "Composite right/left-handed metamaterial antennas," *Antenna Tech. Small Antennas and Novel Metamaterials*, 404–407, 2006.
5. Caloz, C., A. Sanada, and T. Itoh, "A novel composite right-/left-handed coupled-line directional coupler with arbitrary coupling level and broad bandwidth," *IEEE Trans. on Microwave Theory Tech.*, Vol. 52, No. 3, 980–992, 2004.
6. Catarinucci, L., G. Monti, and L. Tarricone, "A parallel-grid-enabled variable-mesh FDTD approach for the analysis of slabs of double-negative metamaterials," *IEEE Antennas and Propagation Society, AP-S International Symposium (Digest)*, 782–785, 2005.
7. Smith, D. R., W. J. Padilla, D. C. Vier, S. C. Nemat-Nasser,

and S. Schultz, "Composite medium with simultaneously negative permeability and permittivity," *Phys. Rev. Lett.*, Vol. 84, No. 18, 4184–4187, May 2000.

8. Monti, G. and L. Tarricone, "On the propagation of a Gaussian pulse in a double-negative slab," *Proc. of 35th European Microwave Conference*, 1419–1422, 2005.
9. Ziolkowski, R. W., "Pulsed and CW Gaussian beam interactions with double negative metamaterial slabs," *Opt. Exp.*, Vol. 11, No. 7, 662–681, Apr. 2003.
10. Monti, G. and L. Tarricone, "A novel theoretical formulation for the analysis of the propagation of finite-bandwidth signals in a double-negative slab," *Microwave and Optical Technology Letters*, Vol. 47, No. 5, 434–439, 2005.
11. Monti, G. and L. Tarricone, "Gaussian pulse expansion of modulated signals in double-negative slab," *IEEE Trans. on Microwave Theory Tech.*, Vol. 54, No. 6, 2755–2761, 2006.
12. Saenz, E., A. Cantora, I. Ederra, R. Gonzalo, and P. de Maagt, "A metamaterial T-junction power divider," *IEEE Microwave and Wireless Components Lett.*, Vol. 17, No. 3, 172–174, Mar. 2007.
13. Monti, G. and L. Tarricone, "Dispersion analysis of a planar negative group velocity-transmission line," *Proceedings of the 37th European Microwave Conference, EUMC*, 1644–1647, 2007.
14. Lin, I-H., C. Caloz, and T. Itoh, "A branch-line coupler with two arbitrary operating frequencies using left-handed transmission lines," *IEEE MTT-S Dig.*, Vol. 1, 325–328, 2003.
15. Monti, G. and L. Tarricone, "Dual-band artificial transmission lines branch-line coupler", *Int. Journal of RF and Microwave Computer-Aided Engineering Wiley*, Vol. 18, No. 1, 53–62, Sep. 2007.
16. Monti, G. and L. Tarricone, "Reduced-size broadband ATL-CRLH rat-race coupler," *Proc. 36th European Microwave Conf.*, 125–128, 2006.
17. Monti, G. and L. Tarricone, "Compact broadband monolithic 3-dB coupler by using artificial transmission lines," *Microwave and Optical Technology Letters*, Vol. 50, No. 10, 2662–2667, 2008.
18. Eccleston, K. W., L. Fan, and S. H. M.Ong, "Compact planar microstripline branch-line and rat-race couplers," *IEEE Trans. on Microwave Theory Tech.*, Vol. 51, No. 10, 2119–2125, 2003.
19. Corchia, L., G. Monti, and L. Tarricone, "MEMS-reconfigurable bandpass filter," *Microwave and Optical Technology Letters*, Vol. 50, No. 8, 2096–2099, 2008.